Determination of carbide structures on an Mo(110) surface by scanning tunneling microscopy and low energy electron diffraction

2008 J. Phys.: Condens. Matter 20 135004

(http://iopscience.iop.org/0953-8984/20/13/135004)

J. Phys.: Condens. Matter **20** (2008) 135004 (6pp) doi:10.1088/0953-8984/20/13/135004

Determination of carbide structures on an Mo(110) surface by scanning tunneling microscopy and low energy electron diffraction

De-Wei Yu, Yi-Hsueh Wu, Rong-Bin Lin and Rong-Li Lo[1]

Department of Physics, National Tsing-Hua University, Hsinchu 300, Taiwan

E-mail: rllo@phys.nthu.edu.tw

Received 10 January 2008
Published 4 March 2008
Online at stacks.iop.org/JPhysCM/20/135004

Abstract

Surface properties of transition metals can be modified considerably by forming carbide overlayers. In this study we fabricated molybdenum carbide overlayers by carburizing the Mo(110) surface with ethylene (C_2H_4) and successfully determined their real space structures by using low energy electron diffraction (LEED) and scanning tunneling microscopy (STM). With various carburization recipes, three carbon-terminated structures $\begin{pmatrix} 5 & 0 \\ -2 & 6 \end{pmatrix}$, (12 × 4)-2C, and (4 × 4) of coverages 1/30, 1/24, and 1/16 monolayer (ML) were formed on the surface, respectively. Since the carbide overlayers were formed at high temperatures, inward diffusion of carbon atoms played a key role in structure formation.

(Some figures in this article are in colour only in the electronic version)

1. Introduction

Owing to the unique bonding structure of the combination of covalent, ionic, and metallic bonds, transition metal carbides (TMCs) are important and interesting materials [1]. TMCs not only have the properties of transition metals, such as high melting point and good thermal conductivity, they also have stable structures of sub-stoichiometry which is one of the characteristics of ceramic. Moreover, TMCs are potential and cheap catalysts because they possess catalytic similarities to noble metals, such as Pd, Pt, Rh, Ru, Ir, and Os [1]. Therefore, TMCs have attracted intense interest in fundamental research and applications in material science in the past few decades.

In the literature, most of the investigations of TMCs focus on the carbide overlayers grown on metal surfaces by carburizing the metal surfaces with C-containing gases because of the scarcity of carbide single crystals. Like the surfaces of metal oxide, complex structures are formed on the carburized metal surfaces due to the variation of C coverage and the coexistence of different structures of multiple domains. Without the unraveling of such complex surface structures, difficulties in data interpretations and the associated insufficiently accurate conclusions may occur. One of the examples is the (4 × 4) carbide overlayer on an Mo(110) surface. Although the surface reactivity of this overlayer has been investigated intensely [2], its exact structure in real space remains unknown so far [3]. In this report, combining STM with LEED we succeeded in determining the real space structures of the carbide overlayers formed on the Mo(110) surface. As the surface C coverage was increased, three structures $\begin{pmatrix} 5 & 0 \\ -2 & 6 \end{pmatrix}$, (12 × 4)-2C or $\begin{pmatrix} 4 & 0 \\ -2 & 6 \end{pmatrix}$, and (4 × 4) were formed. Our results might shed light on the further understanding of the properties of Mo carbide overlayers.

2. Experimental details

A Mo(110) single crystal of diameter 10 mm and thickness 1 mm (99.99%, MaTecK, Germany) was cut into a piece of size of 5 × 3 mm^2. Extended parts on the ledges of a rectangular Ta foil were used as clamps to hold the cut crystal onto the foil. The Ta foil-held sample was mechanically mounted on a commercial STM (Omicron) sample plate. Sample heating was fulfilled by passing a DC current through a pyrolytic boron nitride (PBN) heater beneath the sample, and the

[1] Author to whom any correspondence should be addressed.

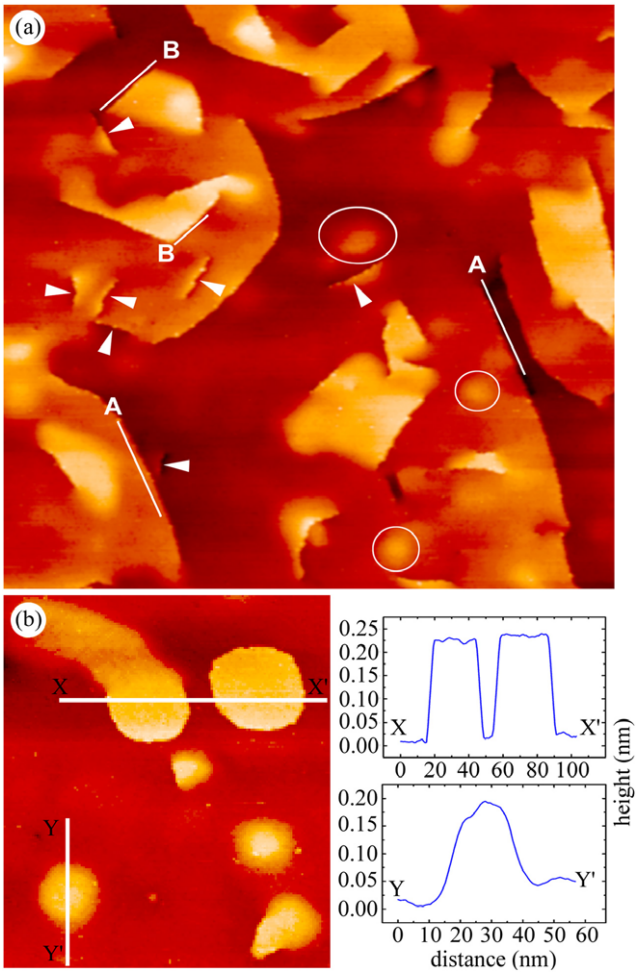

Figure 1. STM images of Mo(110) surface. (a) On an area of 300×300 nm^2 several kinds of surface defects appeared. The segmental steps with subatomic step height are marked by arrows. The other steps are monatomic steps. Short bumps are circled. Directions A and B are probably along the close-packed directions. (b) A monolayer adatom island (upper-right) was formed near local protruded regions. Line profiles of monatomic island (X–X′) and bump (Y–Y′) are presented on the right of the image. Imaging conditions for (a) and (b) are 500 mV/0.5 nA and −300 mV/0.5 nA.

temperatures were read from the heater's power–temperature curve, which was pre-calibrated by a Chromel/Alumel (K type) thermocouple. Cleaning of the Mo(110) substrate was carried out by cycles of 3 keV Ar^+ sputtering in a treatment chamber (base pressure 1.5×10^{-9} Torr), with the ion beam at an angle of 30° to the surface normal, and annealing at 1050 K in an image chamber (base pressure 1.0×10^{-10} Torr) until a sharp Mo(110)-(1 × 1) LEED pattern was obtained. Subsequently, the clean Mo(110) surface was carburized by exposing the Mo(110) surface to C_2H_4 of pressure in the range 10^{-8} Torr at room temperature (RT) or at 800 K, followed by annealing at 1050 K for 10–30 min. Such a carburization recipe was similar to the previous result [4] in which the formation of the carbidic state of carbon atoms is confirmed by Auger electron spectroscopy (AES). When the sample was cooled down to RT, STM images and LEED patterns were taken subsequently

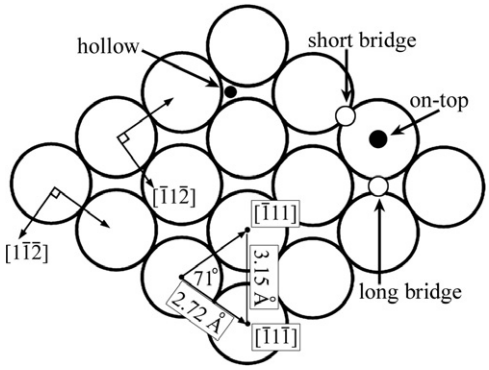

Figure 2. Atomic model of the Mo(110) surface. There are four types of adsorption sites: on-top, short-bridge, long-bridge, and hollow sites. The acute angle between close-packed directions [1̄11] and [1̄11̄] is 71°.

in the image chamber. Electrochemically etched W tips were used in the STM experiments. Before being brought to scan the surface, the etched tips were bombarded by Ar ions to remove the oxides on the tip surface. To obtain high resolution STM images, the tip apex was modified by applying voltage pulses across the surface–tip gap [5].

3. Results and discussion

3.1. Surface morphology

We first examined the morphology of the surface without a carbide overlayer by STM. Figure 1(a) is an STM image of the Mo(110) surface which was acquired after the sample cleaning process. In general, there were two types of surface defect, steps and local protruded regions. Interestingly, a large fraction of steps was formed as segments of height ranging from 0.10 to 0.22 nm, where 0.22 nm is the monatomic step height on the Mo(110) surface [6]. In particular, the heights of the segmental steps marked by arrows in figure 1(a) were less than 0.18 nm. A certain number of straight steps of monolayer height were along the directions A and B shown in figure 1(a). The misaligned angle between these two directions was about 71°. Thus, the directions parallel to A and B were postulated to be the close-packed directions [1̄11] and [1̄11̄] of Mo(110) surface, which are shown in the model in figure 2 [7]. A segmental step of monolayer height resembled the linkage of two screw dislocations of opposed directions, and it usually formed as a part of the border of a local protruded region. Without segmental step-like borders, the bumps indicated by circles in figure 1(a) were classified as one kind of local protruded region. As shown in the line profile YY′ in figure 1(b), the bumps had the size of tenths of nanometers in diameter and a smooth change in height. We also found that not all of the bumps appeared in spherical symmetry. The local protruded regions formed at various heights up to a maximum value of 1 ML. In addition, monolayer islands were found occasionally, as shown in figure 1(b). It seems that the formation of the monolayer island was related to the evolution of a local protruded region

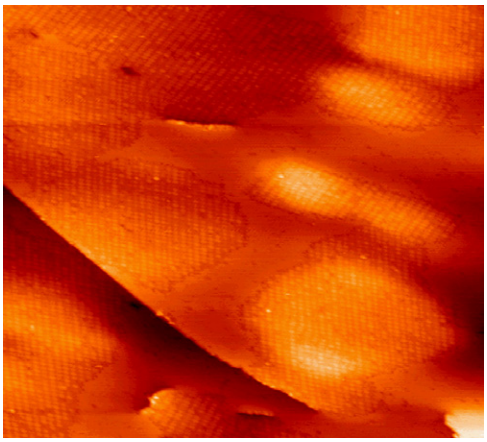

Figure 3. STM image (100 × 90 nm^2, −500 mV/0.3 nA) of the carburized Mo(110) surface. Carburization conditions: exposure of 1.5 L C_2H_4 at RT, followed by annealing to 1050 K for 10 min.

at high temperature when the segmental steps at the perimeter developed into a connection.

It has been well confirmed by the studies of transmission electron microscopy that a bulk experiencing the bombardment of rare gas ions and subsequent moderate high-temperature annealing will bring about the formation of dislocations and gas bubbles, which are formed due to the recrystallization of displaced atoms and thermal accumulation of rare gas atoms implanted during the bombardment process [8, 9]. Both the dislocations and subsurface inert gas bubbles generate surface defects when they interact with the surface. More recently, the surface defects induced by dislocations and subsurface gas bubbles have been observed by STM on face-centered cubic (fcc) metal surfaces. Typical examples are fractional-height segmental steps on Au(111) [10], Au(100) [11], and $Pt_{25}Ni_{75}$(111) [12] surfaces, local protruded regions with borders of segmental steps on Au(100), Ag(100) [11, 13], and Pt(111) [14] surfaces, and bumps and monolayer islands on the Pt(111) surface [14]. However, to our best knowledge, the STM observations of these surface defects have not been reported on a body-centered cubic (bcc) metal surface so far. The most likely formation mechanisms for these surface defects are the intersection of dissociated dislocations with the surface and the punching of dislocation loops driven by overpressurized subsurface gas bubbles [10–14]. The former mechanism produces fractional-height segmental steps, while the latter one generates monolayer islands and local protruded regions of height not taller than 1 ML. In comparison to the results of fcc metal surfaces, our STM observations on the Mo(110) surface seemed more complicated because all types of defect were formed on the surface. The variety of dislocation-induced surface defects on the Mo surface might result from the intersection of the (110) surface with the energetically favored slip planes {110} and {112} [15].

3.2. Ordered structures of carbide overlayer

Figure 3 is a typical STM image of a carburized surface which was obtained by exposing the Mo substrate to about 1.5 L (1 L = 10^{-6} Torr s) of C_2H_4 at RT, followed by annealing to 1050 K for 10 min. As revealed in the image, several districts of ordered structure were generated on the surface. The region distributed among these ordered structures was confirmed to be the incompletely carburized Mo(110) substrate because its area was inversely proportional to the exposure of ethylene. The surface defects shown in figure 1 survived the carburization process. Moreover, owing to the associated local strain and, thus, the higher reactivity to bond with foreign atoms [16, 17], the protruded regions were the preferred places for carbide structures to be generated. The ordered structures shown in figure 3 obviously possessed two misaligned domains. This clue was significantly helpful to interpret the corresponding complex LEED patterns.

A superlattice structure on the surface depends on the coverage of adsorbate. As the exposure of ethylene was increased, three LEED patterns of the carburized surface appeared. They are shown in figures 4(a)–(c) in the order of low to high exposure. Figure 4(a) is the distinguishable LEED pattern when the exposure was less than 2 L at 800 K, and the sharper pattern, figure 4(b), resulted from the exposures above 2 L and less than 9 L. Figure 4(c) is the (4 × 4) pattern that appeared when the exposure was above 9 L at 800 K. Both the patterns in figures 4(a) and (b) possessed 2*mm* symmetry and bore a resemblance to each other. However, at a first glance the main difference between them was the distribution of diffraction spots between the (−10) and (01) beams. In figure 4(b) there were three sharp diffraction spots with equal separation and intensity on the line connecting the (−10) and (01) beams, just the same as those of the (4 × 4) pattern in figure 4(c), whereas this feature was not presented in figure 4(a). These two structures have not been reported before and their complexity in the LEED pattern was ascribed to the combination of diffractions from two misaligned domains, as illustrated in the following STM results.

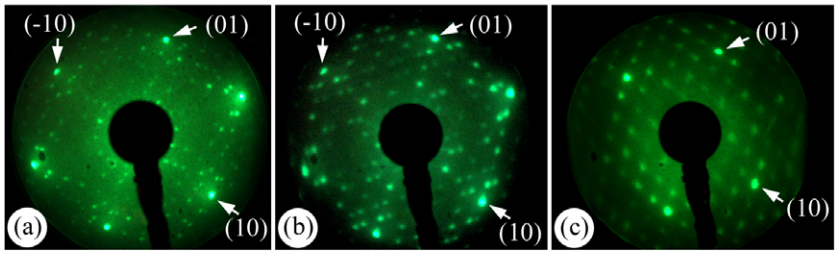

Figure 4. The C_2H_4 dose-dependent LEED patterns from low to high exposure. The patterns in (a)–(c) were from the structures of double domain $\begin{pmatrix} 5 & 0 \\ -2 & 6 \end{pmatrix}$ (E_p = 70 eV), double domain $\begin{pmatrix} 4 & 0 \\ -2 & 6 \end{pmatrix}$ (E_p = 67 eV), and (4 × 4) (E_p = 96 eV), respectively.

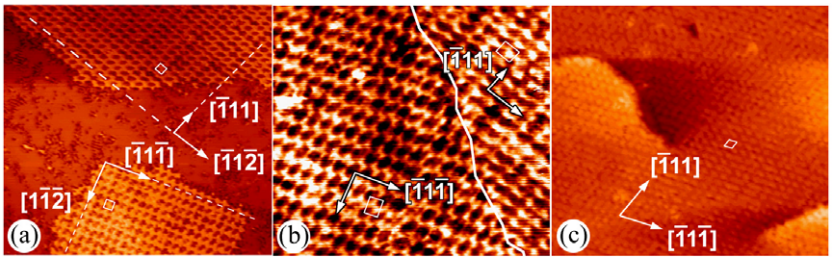

Figure 5. The STM images corresponding to the LEED patterns in figure 4. The unit cell for each structure is depicted and its size is stated in the text. In (a) the upper is $\begin{pmatrix} 6 & -2 \\ 0 & 5 \end{pmatrix}$ and the lower is $\begin{pmatrix} 5 & 0 \\ -2 & 6 \end{pmatrix}$. In (b) the left is $\begin{pmatrix} 4 & 0 \\ -2 & 6 \end{pmatrix}$ and the right is $\begin{pmatrix} 6 & -2 \\ 0 & 4 \end{pmatrix}$, they merged together and formed an irregular domain boundary. (c) is the (4×4) structure. Imaging conditions: (a) −550 mV/0.3 nA, (b) 84 mV/2.0 nA, and (c) −372 mV/0.3 nA.

The STM images corresponding to the LEED patterns displayed in figures 4(a)–(c) are shown in figures 5(a)–(c), respectively. Similar to the α-$Mo_2C(0001)$ surface [18–20], the chemisorbed C atoms appear as depressions in figures 5(a) and (b). However, the image contrast might be inverted, and, thus, C atoms appear as protrusions in figures 3 and 5(c) due to the attachment of different atoms onto the tip apex. We will discuss this later. In the image of the (4×4) structure shown in figure 5(c) the distances between neighboring protrusions along the densely-packed directions [$\bar{1}$11] and [$\bar{1}$1$\bar{1}$] were 1.09±0.04 nm and 1.07±0.04 nm. Both values coincided well with four times the lattice constant of Mo(110)-(1×1) shown in figure 2. The structures presented in figures 5(a) and (b) had rectangular unit cells and two domains rotationally misaligned by around 71°. The twin domains might be separated by an uncarburized area (figure 5(a)) or merged by forming an irregular domain boundary (figure 5(b)). In figure 5(a), the measured distances between neighboring C atoms along [$\bar{1}$11] and [$\bar{1}\bar{1}$2] directions are 1.32 ± 0.02 and 1.53 ± 0.01 nm, respectively, while these distances change to be 1.09 ± 0.01 and 1.54 ± 0.01 nm in figure 5(b). The value 1.32 ± 0.02 nm is close to 1.35 nm, which is five times the lattice constant of Mo(110)-(1×1).

According to the LEED and STM results, we proposed the real space structures for the three ordered overlayers in the top panels of figure 6. The corresponding LEED patterns, which were based on kinematic approximation, were sketched below the atomic models. On the C-terminated surface, C atoms were proposed to be chemisorbed at the hollow site (figure 2) which is similar to the three-fold site on α-$Mo_2C(0001)$ [18–21]. For guidance of the eye, the C atoms are placed on top of Mo atoms. The structure in figure 6(a) had a rectangular unit cell of lattice constants 1.36 and 1.54 nm and two 71°-misaligned domains $\begin{pmatrix} 5 & 0 \\ -2 & 6 \end{pmatrix}$ and $\begin{pmatrix} 6 & -2 \\ 0 & 5 \end{pmatrix}$, and in its resulting LEED pattern (bottom panel) the diffraction spots from different domains did not overlay. Although some spots were too faint to be visible, the distribution of spots between the substrate beams in the observed pattern figure 4(a) agreed well with this proposed pattern. Similarly, the structure in figure 6(b) also had two 71°-misaligned domains $\begin{pmatrix} 6 & -2 \\ 0 & 4 \end{pmatrix}$ and $\begin{pmatrix} 4 & 0 \\ -2 & 6 \end{pmatrix}$, and the lattice constants for its rectangular unit cell were 1.09 and 1.54 nm. The Wood's notation [22] for this structure was Mo(110)–(12×4)-2C. In the resulting LEED pattern (bottom panel), 7/39 of the diffraction spots from one domain overlapped with the spots from the other domain (substrate beams were not included). These overlapping spots are depicted by triangles in the resulting LEED pattern and expected to show up with stronger intensity than the others. Our observed LEED pattern figure 4(b) was consistent with this situation. The increasing C coverage of figure 6(a), 1/30 ML, to figure 6(b), 1/24 ML, also matched the increasing exposure of ethylene. Figure 6(c) shows the proposed (4×4) structure with C coverage 1/16 ML which is much lower than the previous values of 0.3 measured by AES [2, 4]. The discrepancy might be ascribed to the variant detecting depth between STM and AES.

The adsorbed species on the STM tip apex dominates the appearance of the shape of adsorbate as well as the image contrast considerably [23]. Moreover, chemically different adsorbates can also be discriminated by an STM tip whose apex is adsorbed by a special atom or molecule [24, 25]. In our STM experiments the image contrast might be inverted and, in some cases, the image resolution was enhanced significantly when the scanning tip picked up C atoms accidentally from the carbide surface. Scanned by a metal tip, the chemisorbed C atoms on a carburized surface appeared as protrusions, as shown in figure 7(a). In the middle of figure 7(b), transfer of C atoms to the tip apex took place due to an accidental contact of the tip with the surface. When the surface was scanned by a C-tip (the upper half of figure 7(b)), a chemisorbed C atom appeared as a dark spot or a sombrero-like depression, as reported in the α-$Mo_2C(0001)$ surface [18–20].

Because C atoms diffuse into the Mo bulk significantly above 750 K [26], transformation of a high carbon coverage structure into a lower one is feasible by means of additional annealing at 1050 K. As the annealing time was increased, a (4×4) LEED pattern was observed to be transformed into a mixture of (4×4) and (12×4)-2C patterns, followed by a (12×4)-2C pattern and lastly a Mo(110)-(1×1) pattern. Coexistence of different structures, for example in figure 7 the structure $\begin{pmatrix} 5 & 0 \\ -2 & 6 \end{pmatrix}$ (left) is adjacent to the structure (12×4)-2C (right), was observed frequently on the surface. This situation, together with the imperfection of surface morphology, increases the complexity of LEED patterns substantially. In the literature, the perfect (4×4) LEED pattern is usually produced by several cycles of heavy dose of C_2H_4 and annealing at temperatures above 1200 K for short periods [4, 26]. Such recipes would generate a much flatter surface because the local protruded

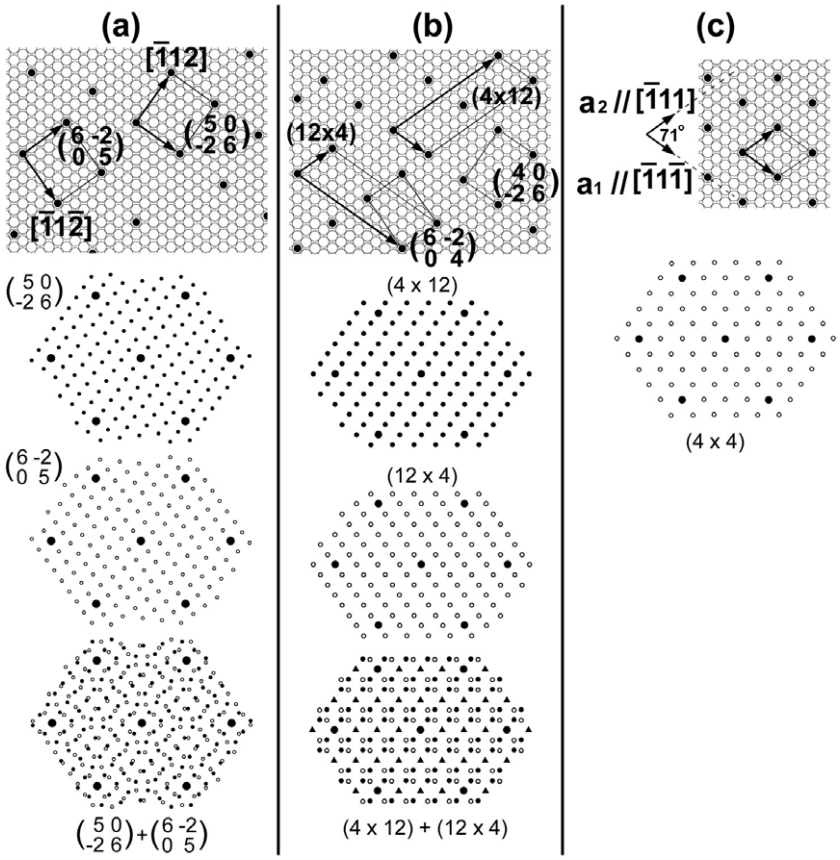

Figure 6. Atomic models and the corresponding LEED patterns for the ordered carbide structures. In the topmost atomic models, for guidance of the eye, C atoms (filled circles) are placed on top of Mo atoms, though C atoms were proposed to be chemisorbed at the hollow site. The large filled circles in the LEED patterns (panels below atomic models) are the substrate spots. The resulting LEED patterns are presented in the lowest panels. In (a) the spots from different domains are separated, while in (b) a fraction of the spots from different domains overlap and are depicted by triangles.

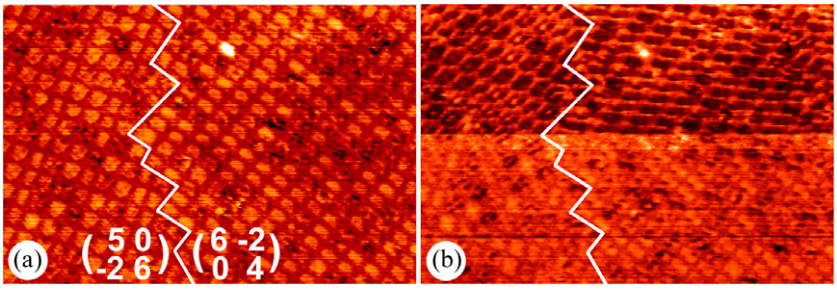

Figure 7. Tip-dependent STM images of carbide structure. (a) A metal tip was used for imaging. (b) A C-tip was formed after a gentle touch to the surface in the middle. The slow scanning direction was from down to up. Imaging conditions: (a) 16 mV/5.0 nA and (b) 30 mV/1.0 nA.

regions and segmental steps vanished under high-temperature annealing [12, 14]. Although the treatment of sample surface employed in fundamental research is required to make the surface morphology as perfect as possible, the imperfection of crystal surface is unavoidable practically. Our carburization recipes not only produced the representative (4 × 4) structure but also the other structures and imperfect surface features not reported before.

With the C_2H_4 exposure up to 240 L, we found no other structures except the observed three structures on the Mo(110) surface. In other words, the maximum number of surface C atoms that the Mo(110) surface could keep was 1/16 ML, which was much lower than 1/3 or 1/2 ML of ordered structures on the surface of single crystal α-Mo_2C(0001) [18–20]. This deviation was ascribed to the fact that C atoms in α-Mo_2C(0001) bulk carry out an outward diffusion to the surface in the process of annealing when the deficiency of surface C atoms occurs during Ar^+ sputtering. On the other hand, the 'defective' (4 × 4) reported by Roe and Schulz [27], which has a lower C coverage than (4 × 4),

was suggested to be $\begin{pmatrix} 5 & 0 \\ -2 & 6 \end{pmatrix}$ or (12 × 4)-2C structures or a combination of them. Another low C coverage structure $\begin{pmatrix} 3 & 3 \\ -4 & 4 \end{pmatrix}$ reported by Young and Slavin [4] was not observed in our study.

4. Conclusions

After the cleaning process of Ar^+ sputtering and annealing to 1050 K, the morphology of the Mo(110) surface was abundant in segmental steps of fractional monatomic height, dislocations, local protruded regions, and bumps. Formation of these unusual surface defects resulted from the intersections of bulk dislocations with the surface. By carburizing the Mo(110) surface with C_2H_4, three exposure-dependent ordered overlayers were formed. Using LEED and STM, we succeeded in determining these C-terminated overlayers to be $\begin{pmatrix} 5 & 0 \\ -2 & 6 \end{pmatrix}$ (12 × 4)-2C and (4 × 4) structures with C coverages of 1/30, 1/24, and 1/16 ML, respectively. A structure of higher C coverage could be changed into a structure of lower C coverage by additional annealing, indicating that the inward diffusion of C atoms played a crucial role in the formation of carbide overlayer. Although the annealing history-dependent coverage of C atoms on the surface exhibited the disadvantage of the carburized Mo(110) surface in the application of catalysis, unraveling of these carbide structures could provide important information for investigations into Mo carbides.

Acknowledgment

This work was supported by National Science Council of Taiwan under contract number NSC 94-2112-M-007-017.

References

[1] Chen J G 1996 *Chem. Rev.* **96** 1477
[2] Hwu H H and Chen J G 2005 *Chem. Rev.* **105** 185
[3] Frühberger B and Chen J G 1996 *J. Am. Chem. Soc.* **118** 11599
[4] Young M B and Slavin A J 1991 *Surf. Sci.* **245** 56
[5] Lo R-L, Chang C-M, Hwang I-S and Tsong T T 2006 *Phys. Rev.* B **73** 075427
[6] Clark J P G Jr and Friend C M 1999 *J. Chem. Phys.* **111** 6991
[7] Colaianni M L, Chen J G, Weinberg W H and Yates J T Jr 1992 *Surf. Sci.* **279** 211
[8] Williams D B and Carter C B 1996 *Transmission Electron Microscopy: A Textbook for Materials Science* (New York: Plenum)
[9] Carter G and Colligon J S 1968 *Ion Bombardment of Solids* (New York: Elsevier)
[10] Engbæk J, Schiøtz J, Dahl-Madsen B and Horch S 2006 *Phys. Rev.* B **74** 195434
[11] de la Figuera J, González M A, García-Martínez R, Rojo J M, Hernán O S, de Parga A L V and Miranda R 1998 *Phys. Rev.* B **58** 1169
[12] Schmid M, Biedermann A, Stadler H and Varga P 1992 *Phys. Rev. Lett.* **69** 925
[13] de la Fuente O R, Zimmerman J A, González M A, de la Figuera J, Hamilton J C, Pai W W and Rojo J M 2002 *Phys. Rev. Lett.* **88** 036101
[14] Michely T and Comsa G 1991 *J. Vac. Sci. Technol.* B **9** 862
[15] Nabarro F R N (ed) 1979 *Dislocations in Solids* vol 2 (Amsterdam: North-Holland)
[16] Gsell M, Jakob P and Menzel D 1998 *Science* **280** 717
[17] Jakob P, Gsell M and Menzel D 2001 *J. Chem. Phys.* **114** 10075
[18] Lo R-L, Fukui K, Otani S, Oyama S T and Iwasawa Y 1999 *Japan. J. Appl. Phys.* 1 **38** 3813
[19] Lo R-L, Fukui K, Otani S and Iwasawa Y 1999 *Surf. Sci.* **440** L857
[20] Fukui K, Lo R-L, Otani S and Iwasawa Y 2000 *Chem. Phys. Lett.* **325** 275
[21] Clair T P S, Oyama S T, Cox D F, Otani S, Ishizawa Y, Lo R-L, Fukui K and Iwasawa Y 1999 *Surf. Sci.* **426** 187
[22] Van Hove M A, Weinberg W H and Chan C-M 1986 *Low-Energy Electron Diffraction* (Berlin: Springer)
[23] Calleja F, Arnau A, Hinarejos J J, de Parga A L V, Hofer W A, Echenique P M and Miranda R 2004 *Phys. Rev. Lett.* **92** 206101
[24] Ruan L, Besenbacher F, Stensgaard I and Laegsgaard E 1993 *Phys. Rev. Lett.* **70** 4079
[25] Bartels L, Meyer G and Rieder K-H 1997 *Appl. Phys. Lett.* **71** 213
[26] Frühberger B and Chen J G 1995 *Surf. Sci.* **342** 38
[27] Roe C L and Schulz K H 2000 *Surf. Sci.* **446** 254